Acta Biochim Biophys Sin 2014, 46: 420–425 | © The Author 2014. Published by ABBS Editorial Office in association with Oxford University Press on behalf of the Institute of Biochemistry and Cell Biology, Shanghai Institutes for Biological Sciences, Chinese Academy of Sciences. DOI: 10.1093/abbs/gmu015.
Advance Access Publication 27 March 2014

Short Communication

Detection of erythrocytes in patients with Waldenström macroglobulinemia using atomic force microscopy

Junru Liu and Juan Li*

Department of Hematology, The First Affiliated Hospital, Sun Yat-sen University, Guangzhou 510080, China
*Correspondence address. Tel: +86-20-87755766-8831; Fax: +86-20-87333122; E-mail: 13719209240@163.com

The pathological changes of erythrocytes are detected at the nanometer scale, which is important for revealing the onset of diseases and diagnosis. The aim of this study is to examine the ultrastructural changes of erythrocytes in Waldenström macroglobulinemia (WM) at a nanometer scale. Blood samples were collected from two healthy volunteers, two WM patients, and three multiple myeloma (MM) patients when they were first diagnosed. The changes of morphology in the erythrocytes were studied at the nanometer level by high-resolution atomic force microscopy imaging (AFM). Compared with the healthy controls and the MM patients, there were dramatic deformations in the overall shape and surface membrane of the erythrocytes in WM patients. Healthy, pathological WM, and MM erythrocytes could be distinguished by several morphological parameters, including the width, length, length-to-width ratio, valley, peak, peak-to-valley, and R_a. AFM is able to detect the morphological differences in the red blood cells from WM patients, healthy controls, and MM patients. Therefore, the erythrocyte morphology is an important parameter for the diagnosis of WM, which can be used to distinguish WM from MM. The changes of ultrastructure in red blood cells may provide a clue to reveal the mechanism of WM.

Keywords atomic force microscopy; Waldenström macroglobulinemia; multiple myeloma; erythrocyte

Received: December 5, 2013 Accepted: January 26, 2014

Introduction

Waldenström macroglobulinemia (WM) is a B-cell disorder characterized primarily by bone marrow infiltration with lymphoplasmacytic cells, along with the demonstration of a monoclonal immunoglobulin M (IgM) protein [1]. The clinical manifestations of the disorder are hepatomegaly (20%), splenomegaly (15%), and lymphadenopathy (15%) [2]. The most common symptom is fatigue that is related to a normochromic or normocytic anemia, bleeding tendency, and hyperviscosity syndrome including visual impairment, neurological symptoms, and Renault phenomenon. The average age of affected individuals is 63–65 years old. WM is currently incurable and most patients die of disease progression, with a median survival of 5 years [3]. The treatment options include oral alkylators (e.g. chlorambucil), nucleoside analogs (cladribine or fludarabine), and rituximab as single agent or rituximab in combination with cyclophosphamide, bortezomib, nucleoside analogs, thalidomide, or bendamustine [4,5].

Atomic force microscopy (AFM) has become a powerful technique for studying the properties of various materials in surface science, biochemistry, and biology. The first application of AFM in medical diagnostics was in 1992. Researchers observed the changes in the erythrocyte shape after splenectomy [6]. Other researchers used AFM to detect changes in the morphological and biomechanical properties of erythrocytes in type 2 diabetes and elliptocytosis complicating idiopathic thrombocytopenic purpura patients, respectively [7,8]. AFM is a unique technology that offers cell topography analysis at nanometer scale [9]. The information of high-resolution topography is important for cellular systems, since it helps to understand the cell architecture and functions [10–12].

Anemia is the most common clinical manifestation in WM patients because of erythropoiesis suppression, the time span of red blood cells (RBCs) shortening, blood losing, and blood dilution from the increased plasma volume. The median hemoglobin value at diagnosis is 10 g/dl [13]. Anemia is also a major indication that WM patients should be treated. The difference between erythrocytes of multiple myeloma (MM) and erythrocytes of healthy donor has been studied using AFM method [14]. The results showed that the healthy and pathological MM erythrocytes could be distinguished by several morphological parameters, including the width, length, length-to-width ratio, valley, peak, peak-to-valley, standard deviation, and surface fluctuation. However, AFM has not been applied in WM patients. There are a lot of similar characteristics in WM and MM such as M protein in plasma,

tumor cells infiltrating bone marrow, and related tissue–organ damage. However, the characteristic found in WM is monoclonal IgM with the same light-chain type, as the IgM was increased in the serum. The immunophenotype profile of WM appears B lymphocytic characteristics such as CD19, CD20, CD22, and so on. The IgM type is rarely found in MM patients. Compared with IgG and IgA, IgM tends to form five polymers that can easily result in hyperviscosity syndrome. As a result, IgM may produce a greater impact on RBCs. It is very important for clinical implications to distinguish WM from MM.

In the present study, we used AFM to study the erythrocytes in patients with WM and compared their morphology with healthy controls and MM patients. Our aim is to examine erythrocyte morphology in WM at a nanometer scale and to aid WM diagnosis and distinguish it from MM.

Materials and Methods

Sample preparation

Blood samples were collected from two WM patients, three MM patients, and two healthy volunteers who did not smoke or take any medication, and prepared at the Department of Hematology, The First Affiliated Hospital, Sun Yat-sen University. Informed consent was obtained from all the donors prior to sample acquisition in accordance with the principles of the Declaration of Helsinki on Biomedical Research. WM patients were diagnosed prior to the onset of the study according to the previously published criteria [1]. The patients were diagnosed based on the following features: monoclonal IgM gammopathy, and surface IgM^+, $CD19^+$, $CD20^+$, and $CD22^+$ immunophenotype. The patients were required to have the symptomatic MM diagnosed according to the previously published criteria [15].

The blood samples were divided into three different groups: Group 1 (newly diagnosed WM patients), Group 2 (newly diagnosed MM patients), and Group 3 (healthy control group). Blood samples were diluted in phosphate-buffered saline solution (pH 7.4), centrifuged (1006 *g* for 10 min) to obtain the erythrocytes, and examined using AFM. An erythrocyte suspension was dropped onto a glass cover slip and air dried prior to AFM scanning and phase-contrast microscopy.

AFM measurement

An Autoprobe CP AFM (Veeco, Plainview, USA) in contact mode, widely used to measure the topography of cells [12,16,17], was applied to detect the immobilized erythrocytes at room temperature. Gold-coated silicon nitride tips (UL20B; Park Scientific Instruments, Baldwin Park, USA) with a spring constant of 2.5 N/m and a tip diameter of 20 nm were used for the AFM experiments. An optical microscope was used to help select the desired cells and direct the position of the AFM tip. Single-cell imaging was performed for 10 cells of each condition, and each cell was scanned three times. The total area analyzed using AFM was a $10 \times 10\ \mu m^2$. The length (L) and width (W) define the maximum and minimum values of the cell diameter, respectively. The peak-to-valley (R_p–v) represents the difference between the maximum and minimum values of the z coordinate on the surface in the area under examination, and R_a defines the average surface fluctuation of the erythrocyte. All parameters were directly determined using the IP 2.1 software (Veeco).

Statistical analysis

Data are expressed as the mean ± standard error. Statistical analyses were performed using SPSS software version 13.0. Differences in the morphological parameters between the three study groups were analyzed with a one-way analysis of variance. A P value <0.05 was considered to be significantly different.

Results

Clinical characteristics of WM patients

Two WM patients were male, age 54 and 60 years old, respectively. Blood routine test showed that the white blood cells were 6.16 and 7.02×10^9/l, neutrophils (2.06, 4.60×10^9/l), hemoglobin (90, 94 g/l), RBCs (2.96, 3.12×10^{12}/l), platelets (159, 164×10^9/l), mean corpuscular volume (91.9, 93.2 fl), mean corpuscular hemoglobin (30.4, 31.2 g/l). The concentration of plasma IgM was 40 and 76 g/l, plasma total protein (82, 108.3 g/l), albumin (26.1, 31.9 g/l), globulin (50.1, 82.2 g/l), serum calcium (2.34, 2.46 mM), respectively. Bence-Jones protein of blood was negative and urine Bence-Jones protein was positive (free kappa). Serum immune fixed electrophoresis showed monoclonal IgM-κ (**Fig. 1A**). Peripheral blood smear showed that red cells appeared rouleaux-like arrangement (**Fig. 1B**). Bone marrow smears showed 11.5% and 13.5% lymphoplasmacytic cells (**Fig. 1C**). Flow cytometry showed $CD19^+$, $CD20^+$, $CD22^+$, and $sIgM^+$. Based on these clinical data, these patients were diagnosed with WM.

AFM results of erythrocytes in healthy donor

Two healthy volunteers were all male, age 50 and 56 years old, respectively. The morphological properties of the healthy erythrocytes visualized by AFM were shown in **Fig. 2**. The healthy erythrocytes had a characteristic biconcave shape (**Fig. 2A,B**), and the corresponding ultrastructure indicated a composite of membrane protein exhibiting regular nanoscale network (**Fig. 2C**). The particles on the surface of healthy erythrocytes were uniform with a diameter of 10 nm. The statistical data in **Fig. 3** showed that the length, width, peak, valley, peak-to-valley value, and average surface fluctuation are

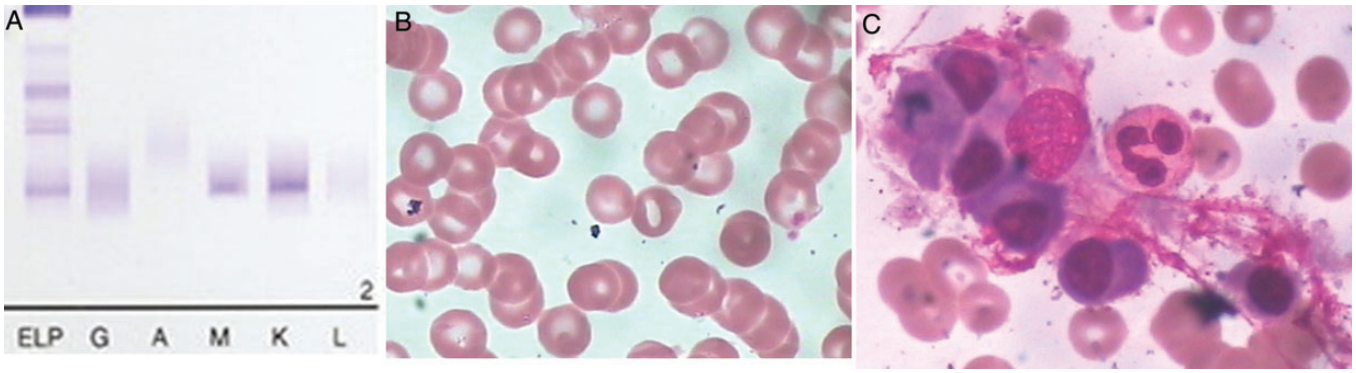

Figure 1. Laboratory information of WM patient (A) Serum immune fixation electrophoresis; (B) blood smear; (C) bone marrow smear.

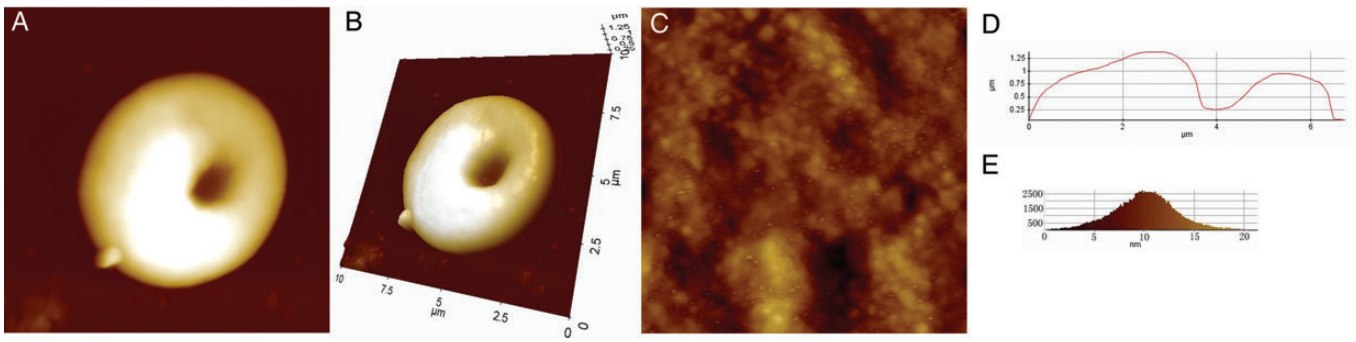

Figure 2. AFM surface topographic image of erythrocyte in healthy donor (A,B) AFM topographic data of single erythrocytes (B are the 3D mode of A). (C) Surface ultrastructure of corresponding cells in images (A) and (B). (D) Height profile of erythrocytes. (E) Histograms of the particle size extracted from images (C). Scanning area: (A) and (B) 10×10 μm^2; (C) 1×1 μm^2.

$L = 6.66 \pm 0.07$ μm, $W = 6.42 \pm 0.06$ μm, $r = 1.04 \pm 0.01$, $H = 1955.33 \pm 49.97$ nm, $h = 42.667 \pm 18.930$ nm, R_p–$v = 1411.0 \pm 24.81$ nm, and $R_a = 231.00 \pm 5.00$ nm, respectively.

AFM results of erythrocytes in WM patients

We first detected the morphological properties of erythrocytes in WM patients using AFM. AFM morphological images of erythrocytes in newly diagnosed WM were shown in **Fig. 4**. The cell surface architecture was extremely deformed, and the center of the cell surface was swollen so that the cells did not exhibit their regular biconcave shape (**Fig. 4A,B**). The position of concave moved from center to the periphery which made the cells irregular. A thorough examination of ultrastructure on the cell surface indicated that there were a number of large ravines and protrusions in the middle of cells (**Fig. 4C**). Compared with the small particles observed in the healthy control erythrocytes (10 nm; **Fig. 2E**), larger particles >40 nm were interspersed on the surface of erythrocytes, implying a significant aggregation of membrane proteins (**Fig. 4E**). The membrane protein was reorganized into a stripe patterns in one direction. These structural abnormalities corresponded to the asymmetric and deformed structure of the erythrocytes. As a result, the defects of the membrane protein and skeleton at molecular scale resulted in the remarkable architecture deformation of erythrocytes.

The topographic images and the corresponding height profiles of single erythrocyte in WM patients (**Fig. 4D**) indicated that the erythrocyte was flat and large in diameter. The statistical data in **Fig. 3** showed that the length, width, peak, valley, peak-to-valley value, and average surface fluctuation of erythrocyte of the WM patients were $L = 7.68 \pm 0.04$ μm, $W = 6.82 \pm 0.06$ μm, $r = 1.13 \pm 0.02$, $H = 1789.333 \pm 561.09$ nm, $h = 265.67 \pm 131.80$ nm, R_p–$v = 1601.33 \pm 400.00$ nm, and $R_a = 292.33 \pm 9.71$ nm, respectively. The values of average length, width, and L/W ratio were significantly higher than those in the healthy erythrocytes (**Fig. 3A**). Roughness, peak (H), and R_p–v of the WM erythrocytes were significantly increased when compared with the healthy erythrocytes (**Fig. 3B**). The larger standard deviations implied more heterogeneous in surface morphology of the WM erythrocytes.

AFM results of erythrocytes in MM patients

Three MM patients were all male, age 55–66 years old. Two of them were IgG type and one was IgA type. AFM morphological images of erythrocytes in newly diagnosed MM were

shown in **Fig. 5**. It was clear that the cell surface architecture was deformed, and the cell surface center also swelled so that the cells did not exhibit their regular biconcave shape (**Fig. 5A,B**). Two little concave-like changes existed in the middle of cell surface. A thorough examination of the cell surface ultrastructure indicated that there were some little holes (**Fig. 5C**). The particles of cell surface were smaller than those of WM erythrocyte with the diameter at 20 nm (**Fig. 5E**). The distribution of particles was very heterogeneous.

The topographic images of single erythrocyte and the corresponding height profiles (**Fig. 5D**) indicated that the erythrocyte was smaller than that of WM in diameter. The statistical data indicated that the length, width, peak, valley, peak-to-valley value, and average surface fluctuation were $L = 6.67 \pm 0.08$ μm, $W = 6.30 \pm 0.06$ μm, $r = 1.06 \pm 0.02$, $H = 1226.67 \pm 230.09$ nm, $h = 342.667 \pm 104.75$ nm, $R_p{-}v = 884.000 \pm 102.68$ nm, and $R_a = 139.67 \pm 85.51$ nm, respectively (**Fig. 3**). The average length, width, and length-to-width ratio were significantly lower than the WM erythrocytes (**Fig. 3A**). Peak-to-valley value ($R_p{-}v$) and R_a of the MM erythrocytes were significantly lower than the WM erythrocytes (**Fig. 3B**).

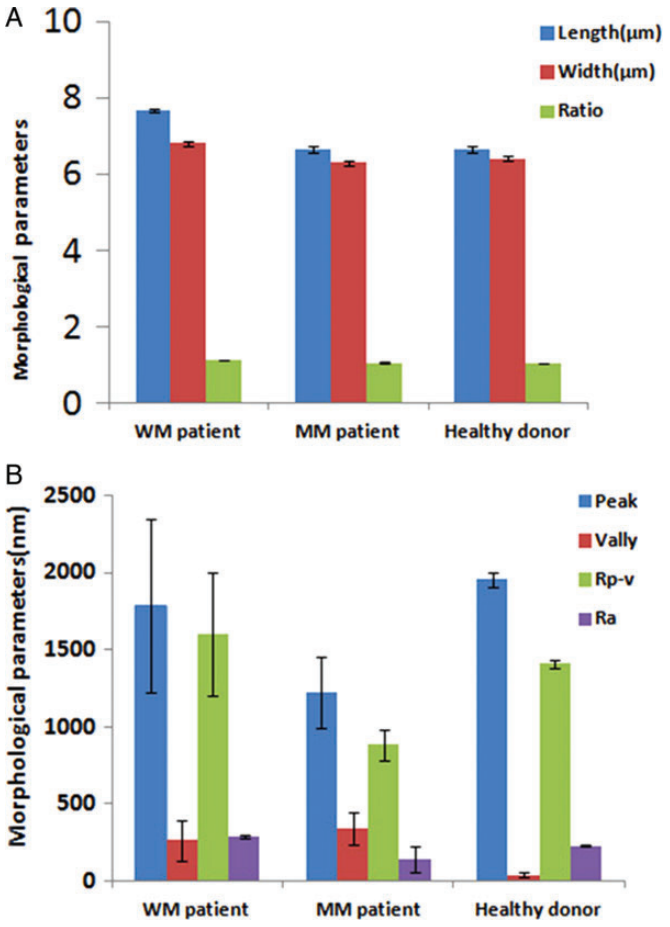

Figure 3. Histograms of erythrocyte morphological parameters (A) Length of L, width of W, ratio of length/width (r). (B) Peak of H, valley (h), peak-to-valley of $R_p{-}v$, and the average surface fluctuation of R_a.

Discussion

Previous clinical studies have indicated that M proteins and the light-chain components of immunoglobulins affect the erythrocytes and enhance the erythrocyte sedimentation ratio [18], which results in RBC aggregation [19]. In WM patients, enhanced erythrocyte aggregation and elevated plasma viscosity were reported. Ramakrishnan *et al*. [20] found that the erythrocyte deformability decreased in the WM patients when compared with the normal adult erythrocytes according to the laser examination. The decrease in deformability of erythrocytes was found to be shear-dependent. Our data indicated that there were obvious morphological difference in erythrocytes between the WM patients and the healthy donor. Similar difference could also exist in erythrocytes between the WM and the MM patients. Jin *et al*. [7] used AFM to detect changes in the morphological and biomechanical properties of erythrocytes in type 2 diabetes. The structural information and mechanical properties of the cell surface membranes of erythrocytes are very important indicators to determine the healthy, diseased, or aging statuses. So, AFM may potentially be developed into a

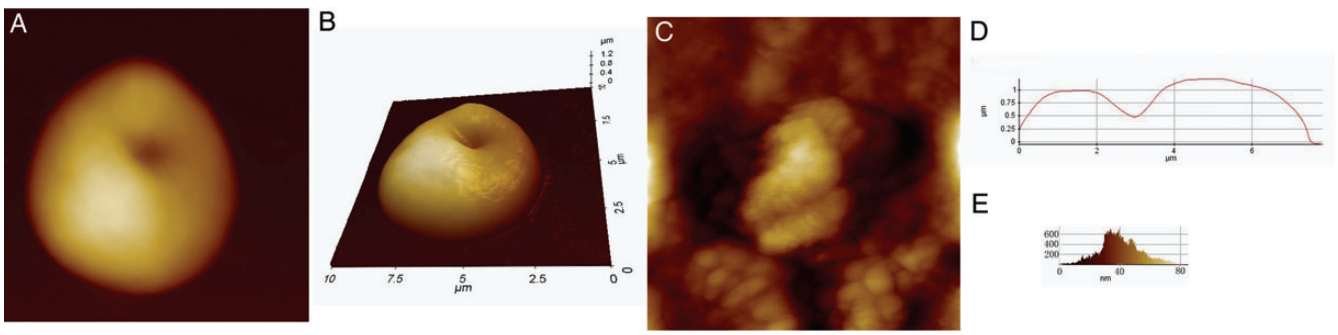

Figure 4. AFM surface topographic image of erythrocyte in WM patients (A,B) AFM topographic data of single erythrocytes (B is the 3D mode of A). (C) Surface ultrastructure of corresponding cells in images (A) and (B). (D) Height profile of erythrocytes. (E) Histograms of the particle size extracted from images (C). Scanning area: (A) and (B) 10×10 μm^2; (C) 1×1 μm^2. WM, Waldenström macroglobulinemia.

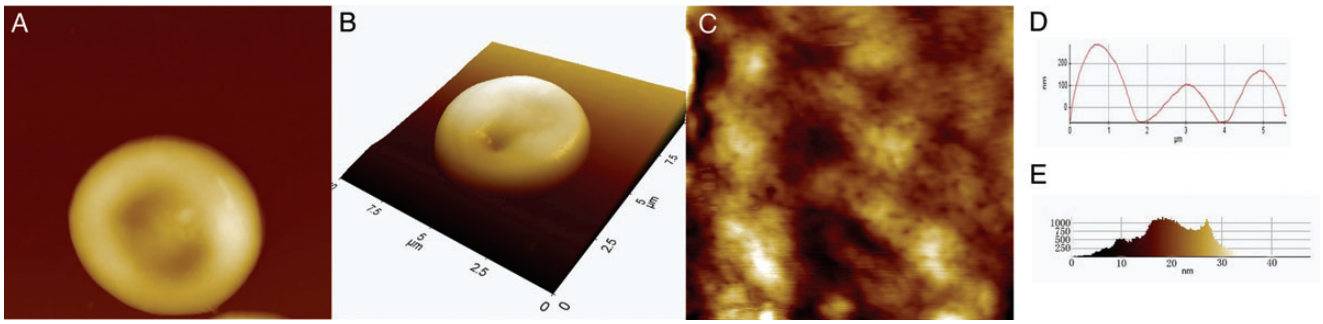

Figure 5. AFM surface topographic image of erythrocyte in MM patients (A,B) AFM topographic data of single erythrocytes (B is the 3D mode of A). (C) Surface ultrastructure on corresponding cells in images (A) and (B). (D) Height profile of erythrocytes. (E) Histograms of the particle size extracted from images (C). Scanning area: (A) and (B) $10 \times 10\ \mu m^2$; (C) $1 \times 1\ \mu m^2$. MM, multiple myeloma.

powerful tool in diagnosing diseases. Other studies also showed that AFM can also be a powerful tool to diagnose iron deficiency anemia, thalassemia, and MM [14,21].

The overall profiles of the healthy erythrocytes appear uniform and have a typical biconcave structure under the optical microscope image. RBCs in patients with newly diagnosed WM appear in a rouleaux-like arrangement and the structure appearing like a normal circle disk was observed under the optical microscopy. The high-resolution AFM image (**Fig. 4A,B**) showed a larger deformability on the membrane surface, and no longer a regular biconcave shape. The structures of the WM erythrocytes were noticeably deformed compared with the healthy erythrocytes. The deformed cells were macrocystic erythrocytes that had a flat shape with a large number of large holes and protrusions on the cell surface. The statistical analysis indicated that the average length, width, and length-to-width ratio were significantly higher than the healthy erythrocytes. Roughness, peak (H), and peak-to-valley value (R_p–v) of the WM erythrocytes were significantly increased compared with the healthy erythrocytes too. Xing *et al*. [8] and Zhang *et al*. [14] reported that the cell center of erythrocytes swells with a subsequent reduction in the peak-to-valley. However, our results showed that the cell center of erythrocytes swells with a subsequent increase in the peak-to-valley in WM. The relationship between the change of cell center and peak-to-valley should be further studied. Because the cell membrane roughness is sensitive to the changes in the membrane-skeleton integrity, R_a can be used to label a whole sample [22]. This difference indicated that the remarkable architecture deformation of the WM erythrocytes may have been induced by the defects in the membrane proteins and skeleton.

Compared with the small particles observed in the healthy control erythrocytes (10 nm; **Fig. 2E**), larger particles >40 nm (**Fig. 4E**) were interspersed on the surface of erythrocytes. This suggested that the membrane protein of WM gathered together and the protein may reorganize to larger particles corresponding to the asymmetry and distortion of structure. Whether the reason for this phenomenon was due to disease itself or to the influence of the IgM package on erythrocytes needs to be further explored. Therefore, the defects of membrane proteins and skeleton at the molecular level cause a great distortion of the structure of RBCs. The abnormal gap on the surface of the red cell membrane structure results in the rupture and deformation of the RBCs. Healthy and pathological WM erythrocytes could be distinguished by several morphological parameters, including the width, length, length-to-width ratio, valley, peak, peak-to-valley, and surface fluctuation.

There are some differences in the erythrocytes between the WM patients and the MM patients revealed by AFM. The morphological changes of MM erythrocytes have already been studied by AFM [14]. The results showed that the length and width of the erythrocytes with the MM were bigger compared with the healthy cells, and the length/width ratio of the pre-therapeutic erythrocytes was larger than the healthy and the post-therapeutic erythrocytes. Our results showed that the length, width, and length/width ratio of the WM erythrocytes were significantly larger than those of the MM erythrocytes. Roughness and R_p–v of the WM erythrocytes were also significantly increased compared with the MM erythrocytes. The average surface fluctuation (292.33 ± 9.71 nm) of WM erythrocytes is about 2 folds that of the MM (139.67 ± 85.51 nm). The particles of cell surface in the MM patients were smaller than those of the WM erythrocyte. WM and MM are mature B-cell neoplasms deriving from post-germinal cells at the different stages of differentiation. Both of them possess the monoclonal immunoglobulin that enhances the erythrocyte sedimentation rate and blood cell aggregation. However, the only type of M protein in WM patients is IgM that is rarely found in the MM patients. IgM in plasma is prone to form five polymers which may exert more influence on erythrocytes compared with IgG or IgA. However, the mechanism still needs to be further studied.

In conclusion, our data indicated that the analysis of erythrocyte morphological parameters may aid WM diagnosis. The noticeable changes in the cellular ultrastructure help us to

better understand the structure–function relationship and the disease pathology of WM. At the nanometer scale, AFM can detect the changes in erythrocyte morphology in the WM, healthy donor, and MM patients. The length, width, length/width ratio, peak, valley, peak-to-valley, and surface fluctuation in the morphological information are important indictors in diagnosing the healthy, WM, and MM. Thus, AFM may be a novel tool to study WM disease. Moreover, the morphological information of the erythrocytes may also serve as a sensitive diseases marker which can reveal the early subtle changes before the significant pathological changes occur.

References

1. Owen RG. Developing diagnostic criteria in Waldenstrom's macroglobulinemia. Semin Oncol 2003, 30: 196–200.
2. Dimopoulos MA and Anagnostopoulos A. Waldenström's macroglobulinemia. Best Pract Res Clin Haematol 2005, 18: 747–765.
3. Vijay A and Gertz MA. Waldenström macroglobulinemia. Blood 2007, 109: 5096–5103.
4. Teeon SP. How I treat Waldenstrom's macroglobulinemia. Blood 2009, 114: 2375–2385.
5. Dimopoulos MA, Gertz MA, Kastritis E, Garcia-Sanz R, Kimby EK, Leblond V and Fermand JP, *et al*. Update on treatment recommendations from the Fourth International Workshop on Waldenstrom's macroglobulinemia. J Clin Oncol 2009, 27: 120–126.
6. Zachee P, Boogaerts MA, Hellemans L and Snauwaert J. Adverse role of the spleen in hereditary spherocytosis—evidence by the use of the atomic force microscope. Br J Haematol 1992, 80: 264–265.
7. Jin H, Xing X, Zhao H, Chen Y, Huang X, Ma S and Ye H, *et al*. Detection of erythrocytes influenced by aging and type 2 diabetes using atomic force microscope. Biochem Biophys Res Commun 2010, 391: 1698–1702.
8. Xing X, Jin H, Lu Y, Wang Q, Pan Y, Cai J and Wang H. Detection of erythrocytes in patient with elliptocytosis complicating ITP using atomic force microscopy. Micron 2011, 42: 42–46.
9. Duvshani-Eshet M, Baruch L, Kesselman E, Shimoni E and Machluf M. Therapeutic ultrasound-mediated DNA to cell and nucleus: bioeffects revealed by confocal and atomic force microscopy. Gene Ther 2006, 13: 163–172.
10. Stolz M, Gottardi R, Raiteri R, Miot S, Martin I, Imer R and Staufer U, *et al*. Early detection of aging cartilage and osteoarthritis in mice and patient samples using atomic force microscopy. Nat Nanotechnol 2009, 4: 186–192.
11. Müller DJ and Dufrêne YF. Atomic force microscopy as a multifunctional molecular toolbox in nanobiotechnology. Nat Nanotechnol 2008, 3: 261–269.
12. Dufrêne YF. Atomic force microscopy and chemical force microscopy of microbial cells. Nat Protoc 2008, 3: 1132–1138.
13. Björkholm M, Johansson E, Papamichael D, Celsing F, Matthews J, Lister TA and Rohatiner AZ. Patterns of clinical presentation, treatment, and outcome in patients with Waldenstrom's macroglobulinemia: a two-institution study. Semin Oncol 2003, 30: 226–230.
14. Zhang Y, Zhang W, Wang S, Wang C, Xie J, Chen X and Xu Y, *et al*. Detection of erythrocytes in patients with multiple myeloma using atomic force microscopy. Scanning 2012, 34: 295–301.
15. Durie BG, Kyle RA, Belch A, Bensinger W, Blade J, Boccadoro M and Child JA, *et al*. Myeloma management guidelines: a consensus report from the Scientific Advisors of the International Myeloma Foundation. Hematol J 2003, 4: 379–398.
16. Lamprecht C, Liashkovich I, Neves V, Danzberger J, Heister E, Rangl M and Coley HM, *et al*. AFM imaging of functionalized carbon nanotubes on biological membranes. Nanotechnol 2009, 20: 434001.
17. Jarosławski S, Duquesne K, Sturgis JN and Scheuring S. High-resolution architecture of the outer membrane of the Gram-negative bacteria *Roseobacter denitrificans*. Mol Microbiol 2009, 74: 1211–1222.
18. Kutulculer N, Karaca NE, Azarsiz E, Aksu G and Gulez N. Immunoglobulin light chain levels can be used to determine disease stage in children with juvenile idiopathic arthritis. Clin Lab Sci 2011, 24: 93–98.
19. Imaizumi K and Shiga T. Effect of immunoglobulins and IgG-fragments on the human erythrocyte aggregation, studied by a rheoscope combined with image analyzer. Biorheology 1983, 20: 569–577.
20. Ramakrishnan S, Degenhardt R and Vietzke K. Erythrocyte deformability in Waldenström's macroglobulinemia. Clin Hemorheol Microcirc 2000, 22: 17–20.
21. Zhang Y, Zhang W, Wang S, Wang C, Xie J, Chen X and Xu Y, *et al*. Detection of human erythrocytes influenced by iron deficiency anemia and thalassemia using atomic force microscopy. Micron 2012, 43: 1287–1292.
22. Girasole M, Pompeo G, Cricenti A, Congiu-Castellano A, Andreola F, Serafino A and Frazer BH, *et al*. Roughness of the plasma membrane as an independent morphological parameter to study RBCs: a quantitative atomic force microscopy investigation. Biochim Biophys Acta 2007, 1768: 1268–1276.